Elimination of electron-ion pseudoresonances associated with approximate target wave functions

T. W. Gorczyca, F. Robicheaux, and M. S. Pindzola
Department of Physics, Auburn University, Auburn, Alabama 36849

D. C. Griffin
Department of Physics, Rollins College, Winter Park, Florida 32789

N. R. Badnell
Department of Physics and Applied Physics, University of Strathclyde, Glasgow, G4 0NG, United Kingdom
(Received 7 July 1995)

One of the problems associated with close-coupling calculations of electron-impact excitation is the occurrence of nonphysical pseudoresonances. These often arise from the $(N+1)$-electron bound states that are routinely kept within the close-coupling expansion. Within the R-matrix formalism, we describe a transformation and reduction of the bound portion of the $(N+1)$-electron basis to eliminate a class of pseudoresonances associated with approximate target wave functions. In order to explain the procedure and demonstrate its effectiveness, we include a variety of examples to show how this method is capable of eliminating those resonances not attached to one of the N-electron states included within the close-coupling expansion of the target.

PACS number(s): 34.80.Kw

I. INTRODUCTION

The collision of electrons with atomic ions constitutes a fundamental process in laboratory and astrophysical plasmas. Electron-impact excitation cross sections in particular serve as important diagnostics for determining the temperature and density of a plasma [1,2]. One of the most powerful computational methods for the generation of electron-ion excitation cross sections is based on the solution of the close-coupling equations [3] through R-matrix theory [4,5]. One of the problems encountered in the standard application of the R-matrix method has been the appearance of pseudoresonance structures in the excitation cross section spectrum. These unphysical structures can be large and sometimes occur in precisely the energy range for which a particular excitation cross-section may have its most useful application in plasma research. In this paper, we introduce a transformation of the bound portion of the scattering wave function, similar in spirit to recent work in electron molecule scattering [6,7], which eliminates a certain class of pseudoresonance structures.

Many times the pseudoresonance structures have their origin in the approximate target wave functions employed. The first example is when only a fraction of the total allowed LS terms within a target configuration are selected for inclusion in the close-coupling expansion. In the case of excitation of Fe^+, this was found to lead to a huge pseudoresonance [8]. The problem may be eliminated by always including all the available LS terms for each target configuration [9]. It would be nice, however, to have the option of selecting the dominant LS terms within a target configuration without worrying about pseudoresonances. A greater freedom in the choice of the target-state wave function for a complex ion would result. A second example is when a pseudo orbital is introduced to take into account orbital variation between different target configurations. In the case of excitation autoionization of Li^+, [10] pseudo orbitals were used to treat 2ℓ orbital variation between the $1s2\ell$ singly excited configurations and the $2\ell 2\ell'$ doubly excited configurations. Although in this case, the pseudoresonances did not occur in the energy region of interest, in general, they will present a problem. A third example is when a pseudo orbital is introduced to take into account the variation of a given bound orbital with the terms of a target configuration. This type of variation is referred to as LS term dependence [11,12]. In the case of excitation autoionization of Kr^{6+} [13], pseudo orbitals were used to treat orbital variation between the ^1S term and all the other LS terms of the $3d^9 4s^2 4d$ target configuration. Pseudoresonances that resulted were found to be present in the $3d \rightarrow 4d$ excitation-autoionization contributions and they limited the accuracy of the ionization cross-section calculations.

The techniques discussed in this paper can be used to eliminate those pseudoresonances associated with states included within the configuration-interaction expansion of the target, but not also included within the N-electron close-coupling expansion. However, when nonphysical states are included in the close-coupling expansion, these techniques cannot be used to eliminate the resonances attached to those states. One example of this is the use of polarized pseudo orbitals within the close-coupling expansion in order to represent the polarization of the target [14]. A second example is the formation of pseudoresonances in the intermediate-energy R-matrix theory [15].

The remainder of this paper is arranged as follows. In order to make clearer the transformation method for eliminating pseudoresonances associated with approximate target wave functions, we start in Sec. II with the classic example of ^1S scattering from hydrogen. The transformation matrix is obtained by inspection of the total wave function. The modifications to the standard R-matrix computer codes needed to eliminate pseudoresonances are outlined in Sec. III. In Sec.

IV we give detailed results for the $1s^2\ ^1S \rightarrow 1s2s\ ^3S$ and the $1s2s\ ^3S \rightarrow 1s2s\ ^1S$ excitations in Li^+ and the $3d^{10}4s^2 \rightarrow 3d^9 4s^2 4d$ excitations in Kr^{6+}. A short summary follows in Sec. V.

II. SCATTERING FROM HYDROGEN

For ^1S scattering from hydrogen, the antisymmetrized, coupled, total wave function is given by

$$\Psi(1sks\ ^1S)=\sqrt{\tfrac{1}{2}}(1s\uparrow,ks\downarrow)-\sqrt{\tfrac{1}{2}}(1s\downarrow,ks\uparrow)\ , \quad (1)$$

where the $\uparrow$ or $\downarrow$ refer to the spin magnetic quantum number and the notation (nl,kl) is used to indicate a two-electron Slater determinant. The bound orbital $P_{1s}(r)$ is not orthogonal to the continuum orbital $F_{ks}(r)$. The Hamiltonian for scattering from hydrogen is given by

$$H=f_1+f_2+g_{12}\ , \quad (2)$$

where f is a one-electron operator representing the kinetic and electron-nuclear energies and g is a two-electron operator representing the Coulomb repulsion energy between the scattered and target electrons. The variational principle applied to the matrix element

$$\langle\Psi|H-E|\Psi\rangle \quad (3)$$

yields

$$\left(f-\frac{k^2}{2}+J^0_{1s}+K^0_{1s}\right)F_{ks}(r)+\left(\epsilon_{1s}-\frac{k^2}{2}\right)\langle P_{1s}|F_{ks}\rangle P_{1s}(r) =0\ , \quad (4)$$

where $J^\kappa_{n\ell}$ and $K^\kappa_{n\ell}$ symbolize direct and exchange operators, ϵ_{1s} is the energy of the $1s$ electron, $k^2/2$ is the energy of the continuum electron, and $\langle P_{1s}|F_{ks}\rangle$ is an overlap integral.

For ^1S scattering from hydrogen, we may also start from a total wave function given by

$$\Psi_S(1s\overline{ks}\,^1S)=\sqrt{\tfrac{1}{2}}(1s\uparrow,\overline{ks}\downarrow)-\sqrt{\tfrac{1}{2}}(1s\downarrow,\overline{ks}\uparrow)+b\chi\ , \quad (5)$$

where

$$\chi=(1s\uparrow,1s\downarrow) \quad (6)$$

and the P_{1s} and $F_{\overline{ks}}$ orbitals are constrained to be orthogonal. The variational principle applied to the expression

$$\langle\Psi_S|H-E|\Psi_S\rangle-\lambda\langle F_{\overline{ks}}|P_{1s}\rangle \quad (7)$$

yields

$$\left(f-\frac{k^2}{2}+J^0_{1s}+K^0_{1s}\right)F_{\overline{ks}}(r)+(\sqrt{2}bJ^0_{1s}-\lambda)P_{1s}(r)=0 \quad (8)$$

from the variation on $F_{\overline{ks}}$ and

$$2\sqrt{2}\langle 1s1s|g|1s\overline{ks}\rangle+2b\left[\epsilon_{1s}-\frac{k^2}{2}+\langle 1s1s|g|1s1s\rangle\right]=0 \quad (9)$$

from the variation on b. The Lagrange multiplier used to force orthogonality between the $F_{\overline{ks}}$ and the P_{1s} orbitals can be determined by multiplying Eq. (8) by P_{1s} and integrating.

In practice, the derivation of the close-coupling equations for a many-electron atomic ion is based on the second method involving Ψ_S. There are two reasons. First, the angular algebra is easier for an orthogonal set of orbitals. With only slight modifications, general computer codes written for bound-state atomic structure can be used to generate the scattering algebra. Second, the nonorthogonal method involving Ψ, even in the case of hydrogen, can lead to uniqueness problems for certain symmetries; ^3S scattering in hydrogen is the classic example. For a many-electron atomic ion this lack of uniqueness can lead to instabilities in the solutions of the close-coupling equations [16].

Unfortunately, the second method involving Ψ_S has problems of its own when applied to many-electron atoms and ions. Nonphysical resonant structures sometimes appear in the cross sections. For this reason, we suggest a third method, which when applied to multielectron systems can eliminate a class of these pseudoresonances. For ^1S scattering from hydrogen the continuum orbital is given by

$$F_{ks}=F_{\overline{ks}}+\beta P_{1s}\ . \quad (10)$$

Upon substitution of Eq. (10) into Eq. (1), the total wave function is given by

$$\Psi_T(1sks\ ^1S)=\sqrt{\tfrac{1}{2}}(1s\uparrow,\overline{ks}\downarrow)-\sqrt{\tfrac{1}{2}}(1s\downarrow,\overline{ks}\uparrow)+\sqrt{2}\beta\chi\ . \quad (11)$$

Thus we see that in this very simple case, the one-component, two-electron, bound portion of Ψ_T can be linked to the one-component, two-electron, bound portion of Ψ_S (i.e., χ) by a trivial, one-to-one transformation matrix $\mathbf{M}=\sqrt{2}$. Instead, we are free to introduce a normalized transformation matrix $\bar{\mathbf{M}}=\mathbf{M}/\sqrt{2}=1$ and the total wave function for the third method is then identical to the wave function of Eq. (5).

In general, the second and third methods outlined above do not give identical descriptions for electron-ion scattering. The third method is found to be superior since it helps to remove problems associated with pseudoresonance structures. In order to demonstrate this, suppose we choose the P_{1s} orbital for ^1S scattering in hydrogen to be that from a Hartree-Fock calculation for the $1s^2$ ground state of neutral helium. To correct for our poor choice for the target wave function, we make a further multiconfiguration Hartree-Fock (MCHF) calculation in which we introduce a $P_{\overline{2s}}$ pseudo orbital and keep the P_{1s} orbital frozen. These calculations were performed using the MCHF package of Froese Fischer [17]. The energy eigenvalue is the exact value of -0.50 a.u., and the mixing coefficients are $c_1=0.9837$ and $c_2=0.1796$. For the second method, the total wave function Ψ_S is given by

$$\Psi_S(1s\overline{ks}\,{}^1S)=\sqrt{\tfrac{1}{2}}c_1[(1s\uparrow,\overline{ks}\downarrow)-(1s\downarrow,\overline{ks}\uparrow)]$$
$$+\sqrt{\tfrac{1}{2}}c_2[(\overline{2s}\uparrow,\overline{ks}\downarrow)-(\overline{2s}\downarrow,\overline{ks}\uparrow)]$$
$$+b_1\chi_1+b_2\chi_2+b_3\chi_3 \ , \qquad (12)$$

where

$$\chi_1=(1s\uparrow,1s\downarrow), \quad \chi_2=\sqrt{\tfrac{1}{2}}[(1s\uparrow,\overline{2s}\downarrow)-(1s\downarrow,\overline{2s}\uparrow)],$$
$$\chi_3=(\overline{2s}\uparrow,\overline{2s}\downarrow) \ , \qquad (13)$$

and the P_{1s}, $P_{\overline{2s}}$, and $F_{\overline{ks}}$ orbitals are constrained to be orthogonal. In the third method, the continuum orbital is given by

$$F_{ks}=F_{\overline{ks}}+\beta_1 P_{1s}+\beta_2 P_{\overline{2s}}. \qquad (14)$$

Upon substitution of Eq. (14) into a modified version of Eq. (1)

$$\Psi(1sks\ {}^1S)=\sqrt{\tfrac{1}{2}}c_1[(1s\uparrow,ks\downarrow)-(1s\downarrow,ks\uparrow)]$$
$$+\sqrt{\tfrac{1}{2}}c_2[(\overline{2s}\uparrow,ks\downarrow)-(\overline{2s}\downarrow,ks\uparrow)] \ , \qquad (15)$$

the total wave function is given by

$$\Psi_T(1sks\ {}^1S)=\sqrt{\tfrac{1}{2}}c_1[(1s\uparrow,\overline{ks}\downarrow)-(1s\downarrow,\overline{ks}\uparrow)]$$
$$+\sqrt{\tfrac{1}{2}}c_2[(\overline{2s}\uparrow,\overline{ks}\downarrow)-(\overline{2s}\downarrow,\overline{ks}\uparrow)]$$
$$+\beta_1(\sqrt{2}c_1\chi_1+c_2\chi_2)$$
$$+\beta_2(c_1\chi_2+\sqrt{2}c_2\chi_3) \ . \qquad (16)$$

By inspection, we see that the transformation matrix that relates the two-component bound portion $\vec{\xi}$ of our two-electron wave function Ψ_T to the three-component bound portion $\vec{\chi}$ of Ψ_S, i.e.,

$$\vec{\xi}=\mathbf{M}\vec{\chi} \ , \qquad (17)$$

is given by

$$\mathbf{M}=\begin{pmatrix} \sqrt{2}c_1 & c_2 & 0 \\ 0 & c_1 & \sqrt{2}c_2 \end{pmatrix} . \qquad (18)$$

The difficulty with this form of Ψ_T is that $\mathbf{M}$ is not an orthonormal transformation matrix. Thus the two bound components ξ_1 and ξ_2 are not orthonormal. Since we want the wave function expanded in an orthonormal basis, we use the following method to generate an orthonormal transformation matrix $\bar{\mathbf{M}}$. We first diagonalize the matrix $\mathbf{B}=\mathbf{M}\mathbf{M}^T$

$$\mathbf{O}^T\mathbf{M}\mathbf{M}^T\mathbf{O}=\mathbf{e} \ , \qquad (19)$$

where the columns of $\mathbf{O}$ are the eigenvectors of $\mathbf{B}$ and the diagonal matrix $\mathbf{e}$ contains the eigenvalues of $\mathbf{B}$. Thus, if we use the matrix $\mathbf{M}'$ defined by the equation

$$\mathbf{M}'=\mathbf{O}^T\mathbf{M} \qquad (20)$$

instead of $\mathbf{M}$ to express the bound portion of Ψ_T in terms of χ_1, χ_2, and χ_3 in Eq. (16), then the two components will be orthogonal with norms equal to e_1 and e_2, respectively. However, if instead we use the matrix $\bar{\mathbf{M}}$ defined by

$$\bar{\mathbf{M}}=\mathbf{e}^{-1/2}\mathbf{O}^T\mathbf{M} \ , \qquad (21)$$

then $\bar{\mathbf{M}}\ \bar{\mathbf{M}}^T=\mathbf{1}$ and the two-component bound portion of Ψ_T will be orthonormal. In this case

$$\mathbf{e}=\begin{pmatrix} 1 & 0 \\ 0 & 2 \end{pmatrix} , \qquad (22)$$

$$\mathbf{O}=\begin{pmatrix} c_2 & c_1 \\ -c_1 & c_2 \end{pmatrix} , \qquad (23)$$

and

$$\bar{\mathbf{M}}=\begin{pmatrix} \sqrt{2}c_1c_2 & c_2^2-c_1^2 & -\sqrt{2}c_1c_2 \\ c_1^2 & \sqrt{2}c_1c_2 & c_2^2 \end{pmatrix} . \qquad (24)$$

The wave function Ψ_T is now given by

$$\Psi_T(1sks\ {}^1S)=\sqrt{\tfrac{1}{2}}c_1[(1s\uparrow,\overline{ks}\downarrow)-(1s\downarrow,\overline{ks}\uparrow)]$$
$$+\sqrt{\tfrac{1}{2}}c_2[(\overline{2s}\uparrow,\overline{ks}\downarrow)-(\overline{2s}\downarrow,\overline{ks}\uparrow)]$$
$$+\beta_1[\sqrt{2}c_1c_2\chi_1+(c_2^2-c_1^2)\chi_2-\sqrt{2}c_1c_2\chi_3]$$
$$+\beta_2[c_1^2\chi_1+\sqrt{2}c_1c_2\chi_2+c_2^2\chi_3] \ , \qquad (25)$$

which is quite different from the wave function of Eq. (12). The variational principle can be used with the wave func-

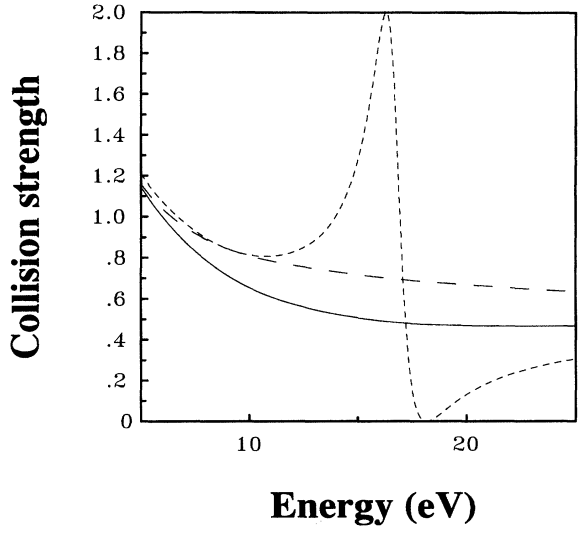

FIG. 1. Collision strength for elastic scattering of electrons from hydrogen in the ^1S partial wave. Short-dashed curve, calculation using the pseudostate wave function of Eq. (12); long-dashed curve, calculation using the pseudostate wave function of Eq. (12) with $b_3=0$; solid curve, calculation using a $1s$ hydrogenic wave function or the pseudostate calculation with the transformed wave function of Eq. (25).

tions of Eqs. (12) and (25) to derive differential equations for the continuum orbital $F_{\overline{\kappa s}}$ similar to Eq. (8).

The elastic collision strength, as a function of incident electron energy, for ^1S scattering from hydrogen is presented in Fig. 1, using the various wave functions derived in the previous paragraphs. The solution of either Eq. (4) or (8) for the elastic phase shifts yields the collision strength presented as the solid curve. The collision strength for the pseudo-orbital case, obtained using the second-method wave function of Eq. (12), is presented as the short-dashed curve. A giant pseudoresonance is found at 15 eV. A widely used approximate scheme to eliminate nonphysical features is to delete χ_3 $(\overline{2s^2})$ from the wave function by setting $b_3=0$ in Eq. (12). The resulting collision strength is shown as the long-dashed curve. Finally, the collision strength obtained using the third-method wave function of Eq. (25) is found to be identical to the previous solid-curve results. Thus the pseudoresonance has been completely eliminated, without affecting the shape of the collision strength.

III. MODIFICATIONS TO THE STANDARD *R*-MATRIX METHOD

We now consider the methods discussed in the preceding section in a more formal way and discuss the modifications of the standard R-matrix method that are necessary to eliminate the pseudoresonances. The $(N+1)$-electron wave function used for a colliding electron incident upon an N-electron atom or ion takes the form [3]

$$\Psi^{N+1}(\mathscr{L}\mathscr{M}_{\mathscr{L}}\mathscr{S}\mathscr{M}_{\mathscr{S}}\Pi)=\mathscr{A}\sum_{L_j,\ell_j,S_j,s_j,\pi_j}\ \sum_{M_{L_j},m_{\ell_j},M_{S_j},m_{s_j}} C^{L_j\ \ell_j\ \mathscr{L}}_{M_{L_j}m_{\ell_j}\mathscr{M}_{\mathscr{L}}}\ C^{S_j\ s_j\ \mathscr{S}}_{M_{S_j}m_{s_j}\mathscr{M}_{\mathscr{S}}}$$
$$\times\Phi^N(L_jM_{L_j}S_jM_{S_j}\pi_j)\phi_{\ell_jm_{\ell_j}}(\vec{r}_{N+1})\zeta_{s_jm_{s_j}}(\sigma_{N+1})\ . \tag{26}$$

In the above equation, the orbital and spin angular momentum quantum numbers and parity for the $(N+1)$-electron wave function, the N-electron target, and the colliding electron are $\{\mathscr{L}\mathscr{M}_{\mathscr{L}}\mathscr{S}\mathscr{M}_{\mathscr{S}}\Pi\}$, $\{L_j,M_{L_j},S_j,M_{S_j},\pi_j\}$, and $\{\ell_j,m_{\ell_j},s_j,m_{s_j},(-1)^{l_j}\}$, respectively. Φ^N denotes the antisymmetrized, coupled wave function for the target electrons and is constructed from linear combinations of Slater determinants formed from N one-electron target wave functions. $\phi_{\ell m_\ell}(\vec{r}_{N+1})$ is the spatial wave function for an incident electron with angular momentum ℓ, which can be written as

$$\phi_{\ell m_\ell}(\vec{r}_{N+1})=F_\ell(r_{N+1})Y^{m_\ell}_\ell(\Omega_{N+1})\ ; \tag{27}$$

$\zeta_{sm_s}(\sigma_{N+1})$ is the wave function for the spin of this electron. The Clebsch-Gordan coefficients C couple the total orbital and spin angular momenta of the target to the orbital and spin angular momenta of the incident electron. Finally, $\mathscr{A}$ is the operator that antisymmetrizes the total wave function upon permutation of the coordinate of the incident electron with the coordinates of the target electrons.

With the R-matrix method [4,5], one expands the radial wave function of the incident electron in a discrete basis of continuum orbitals:

$$F_\ell(r_{N+1})=\sum_i a_{i\ell}v_{i\ell}(r_{N+1})\ . \tag{28}$$

In abbreviated notation then, the R-matrix wave function takes the form

$$\Psi=\mathscr{A}\ \mathscr{C}\sum_{j,\ell_j}\Phi_j\sum_i a_{i\ell_j}v_{i\ell_j}(r)\ , \tag{29}$$

where Φ_j denotes the various target states included in the close-coupling expansion plus the spin and orbital angular momenta of the incident electron and the operator $\mathscr{C}$ denotes the coupling of target and incident-electron angular momenta. These target states are in general some linear combination of configuration-state (CS) functions

$$\Phi_j=Y^{m_{\ell_j}}_{\ell_j}\zeta_{s_jm_{s_j}}\sum_\beta c_{j\beta}\psi_\beta\ , \tag{30}$$

where each CS function ψ_β is a certain coupling of a basic configuration, which can be written in the notation

$$\psi_\beta=n_1\ell_1^{q_1}(\alpha_1L_1S_1)\ \ n_2\ell_2^{q_2}(\alpha_2L_2S_2)L_{12}S_{12}$$
$$\times n_3\ell_3^{q_3}(\alpha_3L_3S_3)L_{123}S_{123}\cdots n_t\ell_t^{q_t}(\alpha_tL_tS_t)LS \tag{31}$$

for t interacting subshells.

As discussed in Sec. II, in the standard R-matrix formulation, the continuum orbitals, and thereby the continuum basis orbitals, are forced to be orthogonal to the target orbitals, i.e., $\langle v_{i\ell}|P_{n\ell}\rangle=0$. This constraint is compensated for by including $(N+1)$-electron bound CS functions, denoted by χ_α, within the close-coupling expansion

$$\Psi_S=\mathscr{A}\ \mathscr{C}\sum_{j,\ell_j}\Phi_j\sum_i a_{i\ell_j}v_{i\ell_j}(r)+\sum_\alpha b_\alpha\chi_\alpha\ . \tag{32}$$

For the simple case when the set of states included in the close-coupling expansion $\{\Phi_j\}$ constitute a unitary representation of the basis of CS functions formed by all couplings of the set of N-electron configurations included in the configuration-interaction expansion, then the basis of $(N+1)$-electron bound CS functions $\{\chi_\alpha\}$ is completely de-

termined. It is the set of all possible $(N+1)$-electron bound CS functions formed by coupling any open-shell one-electron target wave function to all possible target N-electron CS functions ψ_β.

However, it is often true that, for physical or practical reasons, the number of target states included in the close-coupling expansion is smaller than the set of CS functions that can be be formed from the configuration-interaction expansion of the target, i.e., the set of close-coupling target states is not isomorphic to the basis of CS functions used to describe it. Cases may then arise for which no single choice of $(N+1)$-electron bound CS functions $\{\chi_\alpha\}$, is physically correct. Instead, as we saw in Sec. II when the $\overline{2s}$ pseudo orbital is included to describe elastic scattering in hydrogen, only certain linear combinations of these must be retained. In a fashion similar to the derivation of Eq. (16) from Eq. (14), we go back to the original form of the wave function given in Eq. (29) and let the continuum basis include the target orbitals $P_{n\ell}$ as well as the set $v_{i\ell}$, which are orthogonal to these. The wave function now takes the form

$$\Psi_T=\mathscr{A}\ \mathscr{C}\sum_{j,\ell_j}\Phi_j\left(\sum_i a_{i\ell_j}v_{i\ell_j}+\sum_{n_j}\beta_{n_j\ell_j}P_{n_j\ell_j}\right)\ . \tag{33}$$

The second term on the right-hand side of Eq. (33) can be written in terms of the original $(N+1)$-electron bound basis of CS functions $\{\chi_\alpha\}$:

$$\mathscr{A}\mathscr{C}\Phi_jP_{n_j\ell_j}=\mathscr{A}\mathscr{C}\sum_\beta c_{j\beta}\psi_\beta Y^{m_j}_{\ell_j}\zeta_{s_jm_{s_j}}P_{n_j\ell_j}$$

$$=\sum_\gamma M_{k,\gamma}\chi_\gamma\ . \tag{34}$$

The index k denotes all possible combinations of coupling any open-shell, one-electron, target wave function $Y^{m_j}_{\ell_j}\zeta_{s_jm_{s_j}}P_{n_j\ell_j}$ to any target term Φ_j included in the close-coupling expansion. Determining the overlap matrix $\mathbf{M}$ between this inequivalent-electron coupling scheme and the $(N+1)$-electron bound CS functions involves certain recoupling and antisymmetrization steps, which will be illustrated by specific examples in Sec. IV. The key point is that each coupling in Eq. (34) is obviously some linear combination of $(N+1)$-electron bound CS functions.

We now consider how the matrix $\mathbf{M}$ can be determined using existing R-matrix programs. We first introduce a one-electron unit operator $u(r)$ such that it is equal to one when its coordinate is the same as the coordinate of $P_{n_j\ell_j}$ and is equal to zero otherwise; i.e., when applying this operator, we force the bound orbital $P_{n_j\ell_j}$, which is being added to the N-electron target state Φ_j, to be the active electron. Since it is this orbital that will be recoupled to the N-electron target state in the evaluation of the overlap matrix, forcing it to be the active one allows us to evaluate the overlap matrix elements in terms of the matrix elements of this operator, that is,

$$M_{k,\alpha}=\langle\chi_\alpha|\mathscr{A}\mathscr{C}\Phi_jP_{n_j\ell_j}\rangle$$

$$=\sum_\beta c_{j\beta}\left\langle\chi_\alpha\left|\sum_{i=1}^{N+1}u(r_i)\right|\mathscr{A}\mathscr{C}\psi_\beta Y^{m_j}_{\ell_j}\zeta_{s_jm_{s_j}}P_{n_j\ell_j}\right\rangle\ . \tag{35}$$

But since $\langle P_{n_s\ell_s}|u|P_{n_j\ell_j}\rangle=\delta_{n_s,n_j}\delta_{\ell_s,\ell_j}$, then

$$M_{k,\alpha}=\sum_\beta c_{j\beta}\sum_{s=1}^{t}W^s_{\alpha,\beta}\ \delta_{n_s,n_j}\delta_{\ell_s,\ell_j}\ . \tag{36}$$

The index s denotes each of the t open subshells in the $(N+1)$-electron bound CS functions χ_α. However, we can now determine the coefficients $W^s_{\alpha,\beta}$ by using the identical angular weighting factors that occur in the evaluation of one-electron, spherical operators $f(r)$

$$\left\langle\chi_\alpha\left|\sum_{i=1}^{N+1}f(r_i)\right|\mathscr{A}\mathscr{C}\psi_\beta Y^{m_j}_{\ell_j}\zeta_{s_jm_{s_j}}v_{i\ell_j}\right\rangle$$

$$=\sum_{s=1}^{t}W^s_{\alpha,\beta}\langle P_{n_s\ell_s}|f|v_{i\ell_j}\rangle\delta_{\ell_s,\ell_j} \tag{37}$$

and are routinely calculated when constructing the R-matrix Hamiltonian.

Given the overlap matrix $\mathbf{M}$, the expansion in Eq. (33) can be rewritten as

$$\Psi_T=\mathscr{A}\ \mathscr{C}\sum_{j,\ell_j}\Phi_j\sum_i a_{i\ell_j}v_{i\ell_j}(r)$$

$$+\sum_{j,n_j,\ell_j}\beta_{n_j\ell_j}\sum_\alpha M_{k,\alpha}\chi_\alpha\ . \tag{38}$$

The matrix $\mathbf{M}$ has N_r rows and N_c columns, which are not equal in general. If $N_r>N_c$, then a Gaussian elimination of the matrix $\mathbf{M}$ will yield at least N_r-N_c rows in which all elements are zero. We can therefore use an orthonormal transformation of the original basis set $\{\chi_\alpha\}$ for which only N_c rows are needed. Of course, there still may be other rows that are linearly dependent and so the rank of the matrix may be reduced to $N_r<N_c$. For other cases, we may have $N_r<N_c$ to begin with.

We use the method outlined in Sec. II [Eqs. (19)–(21)] to determine the eigenvector matrix $\mathbf{O}$ and the eigenvalue matrix $\mathbf{e}$ for the matrix $\mathbf{B}=\mathbf{M}\mathbf{M}^T$ and thereby the orthonormal transformation matrix $\bar{\mathbf{M}}=\mathbf{e}^{-1/2}\mathbf{O}^T\mathbf{M}$. We choose the eigenvalues to be ordered so that $e_i>e_{i+1}$. These eigenvalues will usually be about 1.0 or 0.0. The reason that the larger ones are not identically one is because inequivalent couplings for an equivalent orbital can (i) lead to zero for certain possible $(N+1)$-electron bound terms due to the antisymmetrization operator $\mathscr{A}$ and (ii) lead to factors greater than one in other $(N+1)$-electron bound terms [e.g., $n\ell n'\ell(^1S)=\sqrt{2}(n\ell)^2(^1S)$ when $n'=n$]. The eigenvalues of zero would correspond to linear combinations of the basis set $\{\chi_\alpha\}$, using the transformation matrix $\mathbf{M}'$ defined by Eq. (20), for which the norm is zero. Therefore, they are not required in the $(N+1)$-electron bound portion of the expansion for

Ψ_T. Those linear combinations corresponding to an eigenvalue somewhat greater than zero are less clearly defined. As a general rule, we keep only those linear combinations corresponding to an eigenvalue greater than 0.01; all others are not required by orthogonality considerations and may lead to pseudoresonances. The number of rows kept N_r is determined by this criterion. In cases where an eigenvalue is larger than 0.01, this indicates that one needs to reconsider the terms retained in the close-coupling expansion. In practice, we have found that in cases for which $e_i \sim 0.01$, there is such strong mixing between those configurations included in the close-coupling expansion and those omitted that these latter configurations really should not be omitted in the first place. A specific example in Sec. IV B will illustrate this point.

It is certainly an approximation to eliminate those linear combinations corresponding to an eigenvalue in the range $0 < e_i \leq 0.01$. However, when this renormalized linear combination is retained, a pseudoresonance may appear. Perhaps a more rigorous method, which compensates for the orthogonality constraints while avoiding pseudo resonances, would be to apply a variational principle to the functional

$$\frac{\langle \Psi_T | H - E | \Psi_T \rangle}{\langle \Psi_T | \Psi_T \rangle} \ . \tag{39}$$

The resulting close-coupling equations then have an extra energy-dependent, nonlocal potential, similar to a Lagrange multiplier, which ensures that those linear combinations that yield a total wave function of zero or close to zero do not accidentally solve the close-coupling equations. In other words, if a variational principle were applied to the functional in Eq. (3) using the nonorthonormal wave function Ψ_T in Eqs. (33) and (34), nonphysical solutions can result simply because the norm of Ψ_T may be close to zero. These nonphysical solutions yield pseudoresonances. The resulting close-coupling equations derived using the functional in Eq. (39) are difficult to solve however. Due to the extra energy-dependent, non-local potential, which depends on the wave function itself, an iterative method is required and this severely complicates the problem. For this reason, we shall not pursue that method further.

To see how the basis $\vec{\bar{\xi}} = \mathbf{M}\vec{\chi}$ may be used with only slight modifications to existing R-matrix methods, we describe a simple transformation of the original Hamiltonian. The original wave function in Eq. (32) can be compactly written as

$$\Psi_S = \vec{\psi}_c{}^T \vec{a} + \vec{\chi}^T \vec{b} \ , \tag{40}$$

where the elements of $\vec{\psi}_c$ are $\mathscr{A}\mathscr{C}\Phi_j v_{i\ell_j}$ and the elements of $\vec{\chi}$ are χ_α. The expectation value of the Hamiltonian is then

$$\int d\vec{r}_1 d\sigma_1 \cdots d\vec{r}_{N+1} d\sigma_{N+1} \{ \ \Psi_S^* \mathscr{H} \Psi_S \ \}$$
$$= (\vec{r}^T \ \vec{b}^T) \begin{pmatrix} \mathbf{H}_{cc} & \mathbf{H}_{cb} \\ \mathbf{H}_{bc} & \mathbf{H}_{bb} \end{pmatrix} \begin{pmatrix} \vec{a} \\ \vec{b} \end{pmatrix} \ . \tag{41}$$

The new basis replaces the second term in Eq. (40) with $\vec{\xi}^T \vec{\beta} = \vec{\chi}^T \bar{\mathbf{M}}^T \vec{\beta}$, so that the Hamiltonian submatrices are transformed as

$$\mathbf{H}_{cc} \leftarrow \mathbf{H}_{cc}, \quad \mathbf{H}_{cb} \leftarrow \mathbf{H}_{cb} \bar{\mathbf{M}}^T,$$

$$\mathbf{H}_{bc} \leftarrow \bar{\mathbf{M}} \mathbf{H}_{bc}, \quad \mathbf{H}_{bb} \leftarrow \bar{\mathbf{M}} \mathbf{H}_{bb} \bar{\mathbf{M}}^T \ . \tag{42}$$

For $N_r < N_c$, the order of the Hamiltonian is reduced. This leads to fewer poles of the matrix $(E - \mathbf{H})^{-1}$ and those that are discarded correspond to pseudoresonances. We now illustrate the applications of the above techniques by considering actual scattering cases.

IV. APPLICATIONS OF THE MODIFIED *R*-MATRIX METHOD

In this section, we consider three different examples, all of which illustrate how the methods of the preceding section can be used to eliminate pseudoresonances. The first case, a model calculation of excitation in Li^+, demonstrates how pseudoresonances corresponding to eigenvalues that are identically zero are removed. Computation of the elements of the transformation matrix $\mathbf{M}$ will be described as well. The second case is similar to the first, except the removed pseudoresonances are associated with eigenvalues that are small but not exactly zero. The third is an actual physical case for which pseudoresonances were previously found to be problematic. The following calculations utilized Froese Fischer's multiconfiguration Hartree-Fock package [17] to generate the target orbitals and a modified version of the R-matrix programs [18] that were coded for the Iron Project [19].

TABLE I. ^2S wave-function description for the $1s^2\ ^1S \rightarrow 1s2s\ ^3S$ transition in Li^+.

Target orbitals $P_{n_j \ell_j}$	Target terms in the set $\{\Phi_j\}$	$(N+1)$-electron CS functions in the set $\{\chi_\alpha\}$
$1s$	$1s^2(^1S)$	$1s^2 2s\ ^2S$
$2s$	$(c_1 1s2s + c_2 1s\overline{3s})(^3S)$	$1s^2\overline{3s}\ ^2S$
$\overline{3s}$		$1s2s^2\ ^2S$
		$1s2s(^1S)\overline{3s}\ ^2S$
		$1s2s(^3S)\overline{3s}\ ^2S$
		$1s\overline{3s}^2\ ^2S$

A. $1s^2\ ^1S \rightarrow 1s2s\ ^3S$ excitation in Li^+

As a first example, we consider the ^2S partial wave for the $1s^2\ ^1S \rightarrow 1s2s\ ^3S$ excitation in Li^+. In this case, we will illustrate not only how a pseudoresonance associated with an N-electron term involving a pseudo orbital can be eliminated from a calculation but also how a pseudoresonance associated with an N-electron spectroscopic term, which is not included in the close-coupling expansion of the target, can be removed. We determined the $1s$ orbital from a Hartree-Fock (HF) calculation on the $1s^2\ ^1S$ term. However, in order to force the use of a pseudo orbital in this calculation, the $2s$ orbital was calculated from a HF calculation for Li^{2+}. We can compensate for this inappropriate $2s$ orbital by performing a MCHF calculation, which includes the $1s2s\ ^3S$ and $1s\overline{3s}\ ^3S$ CS functions. The $\overline{3s}$ pseudo orbital is far from a spectroscopic $3s$ orbital, and the $1s2s\ ^3S$ term is given by the linear combination $(c_1 1s2s\ ^3S + c_2 1s\overline{3s}\ )^3S$, with $c_1 = 0.9640$ and $c_2 = -0.2659$.

The target orbitals $P_{n_j \ell_j}$, the target terms included in the close-coupling expansion in Φ_j, and the $(N+1)$-electron bound CS functions χ_α for the ^2S wave-function description are listed in Table I. Note that there are $N_c = 6$ $(N+1)$-electron bound CS functions and also $N_r = 3(\text{orbitals}) \times 2(\text{target terms}) = 6$ possible $(N+1)$-electron bound terms contained in $\vec{\xi}$, by orthogonality considerations. The nonorthonormal form of $\vec{\xi}$ is related to $\vec{\chi}$ by the overlap matrix **M**

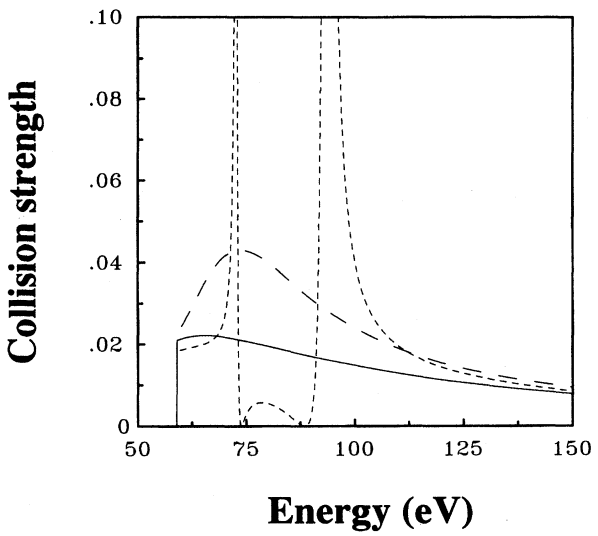

FIG. 2. Electron-impact excitation collision strength for the $1s^2\ ^1S \rightarrow 1s2s\ ^3S$ transition in Li^+ from various two-term R-matrix calculations in the ^2S partial wave. Short-dashed curve, full calculation using all $(N+1)$-electron bound CS functions from Table II; long-dashed curve, calculation omitting the $1s2s(1S)\overline{3s}\ ^2S$ and $1s\overline{3s}^2\ ^2S$ CS functions; solid curve, calculations using either the 2s orbital from a Hartree-Fock calculation on $1s2s\ ^3S$ or the pseudostate calculation with the transformed, reduced basis set. Both the short-dashed curve and the long-dashed curve exhibit unphysical behavior.

$$\vec{\xi} = \begin{pmatrix} 1s^2(^1S)1s \\ 1s^2(^1S)2s \\ 1s^2(^1S)\overline{2s} \\ (c_1 1s2s + c_2 1s\overline{3s})(^3S)1s \\ (c_1 1s2s + c_2 1s\overline{3s})(^3S)2s \\ (c_1 1s2s + c_2 1s\overline{3s})(^3S)\overline{3s} \end{pmatrix}$$

$$= M\vec{\chi} = \begin{pmatrix} 0 & 0 & 0 & 0 & 0 & 0 \\ 1 & 0 & 0 & 0 & 0 & 0 \\ 0 & 1 & 0 & 0 & 0 & 0 \\ -c_1\sqrt{\tfrac{3}{2}} & -c_2\sqrt{\tfrac{3}{2}} & 0 & 0 & 0 & 0 \\ 0 & 0 & c_1\sqrt{\tfrac{3}{2}} & \dfrac{-c_2\sqrt{3}}{2} & \dfrac{c_2}{2} & 0 \\ 0 & 0 & 0 & 0 & c_1 & c_2\sqrt{\tfrac{3}{2}} \end{pmatrix} \begin{pmatrix} 1s^2 2s \\ 1s^2\overline{3s} \\ 1s2s^2 \\ 1s2s(^1S)\overline{3s} \\ 1s2s(^3S)\overline{3s} \\ 1s\overline{3s}^2 \end{pmatrix} . \tag{43}$$

Note that the first row is identically zero, and the fourth row is linearly dependent on the second and third rows, so that a trivial reduction of $N_r = 6$ to $N_r = 4$ may be performed.

As an example of how each matrix element is determined, we focus on the fifth row of **M**, the coupling $(c_1 1s2s + c_2 1s\overline{2s})(^3S)2s\ ^2S$. Here we have assumed that coupling is from left to right, and that the wave functions are antisymmetrized. Using Eq. (36)

$$M_{5,3} = \left\langle 1s(2s^2\ ^1S)^2S \left| \sum_{i=1}^{3} u(r_i) \right| (c_1 1s2s + c_2 1s\overline{3s})(^3S)2s\ ^2S \right\rangle . \tag{44}$$

From Eq. (13.53) of Ref. [12],

$$M_{5,3}=c_1\sqrt{2}\ \langle 1s(r_1)[2s(r_2)2s(r_3)\ {}^1S]^2S|u(r_3)|1s(r_1)2s(r_2)({}^3S)2s(r_3)\ {}^2S\rangle\ ; \tag{45}$$

then using Eq. (13.64) of Ref. [12] to recouple the ket, this becomes

$$M_{5,3}=c_1\sqrt{6}\ (-1)^{1/2+1/2+1/2+1/2}\begin{Bmatrix} \frac{1}{2} & \frac{1}{2} & 1 \\ \frac{1}{2} & \frac{1}{2} & 0 \end{Bmatrix}\langle 1s(r_1)[2s(r_2)2s(r_3)\ {}^1S]^2S|u(r_3)|1s(r_1)[2s(r_2)2s(r_3)\ {}^1S]^2S\rangle\ . \tag{46}$$

However,

$$\langle 1s(r_1)[2s(r_2)2s(r_3)\ {}^1S]^2S|u(r_3)|1s(r_1)[2s(r_2)2s(r_3)\ {}^1S]^2S\rangle=1;$$

therefore

$$M_{5,3}=c_1\sqrt{\tfrac{3}{2}}\ . \tag{47}$$

Now we treat $M_{5,4}$ and $M_{5,5}$ together in the form

$$M_{5,n}=\left\langle 1s2s(^{2(n-4)+1}S)\overline{3s}\ {}^2S\left|\sum_{i=1}^{3}u(r_i)\right|(c_1 1s2s+c_2 1s\overline{3s})({}^3S)2s\ {}^2S\right\rangle, \tag{48}$$

with $n=4$ or 5. Again, from Eq. (13.53) of Ref. [12],

$$M_{5,n}=-c_2\ \langle 1s(r_1)2s(r_3)(^{2(n-4)+1}S)\overline{3s}(r_2)^2S|u(r_3)|1s(r_1)\overline{3s}(r_2)({}^3S)2s(r_3)\ {}^2S\rangle\ . \tag{49}$$

Finally, we use Eq. (13.66) of Ref. [12] to recouple the ket

$$\begin{aligned} M_{5,n}=&-c_2\sqrt{3[2(n-4)+1]}(-1)^{1/2+1/2+(n-4)}\begin{Bmatrix} \frac{1}{2} & \frac{1}{2} & 1 \\ \frac{1}{2} & \frac{1}{2} & (n-4) \end{Bmatrix} \\ &\times\langle 1s(r_1)2s(r_3)(^{2(n-4)+1}S)\overline{3s}(r_2)\ {}^2S|u(r_3)|1s(r_1)2s(r_3)(^{2(n-4)+1}S)\overline{3s}(r_2)\ {}^2S\rangle \\ =&(-1)^{(n-3)}\ \sqrt{\frac{3}{2(n-4)+1}}\ \frac{c_2}{2}\ . \end{aligned} \tag{50}$$

Thus $M_{5,4}=-c_2\sqrt{3}/2$ and $M_{5,5}=c_2/2$.

When we diagonalize the matrix $\mathbf{B}=\mathbf{M}\mathbf{M}^T$, the eigenvalues are

$$e_i=(2.5,\ 1.5,\ 1.0,\ 1.0,\ 0.0,\ 0.0)\ . \tag{51}$$

Thus, in this case, two of the eigenvalues are identically zero, as was easily seen by inspecting the matrix **M,** and we keep only four of the possible six linear combinations of the three-electron states χ_α. The resulting orthonormal $\bar{\mathbf{M}}$ matrix is given by

$$\bar{\mathbf{M}}=\begin{pmatrix} -0.9705 & 0.2413 & 0.0000 & 0.0000 & 0.0000 & 0.0000 \\ 0.0000 & 0.0000 & 0.9418 & 0.1656 & -0.2868 & 0.0582 \\ 0.0000 & 0.0000 & 0.2868 & 0.0504 & 0.9127 & -0.2868 \\ 0.2413 & 0.9705 & 0.0000 & 0.0000 & 0.0000 & 0.0000 \end{pmatrix}\ . \tag{52}$$

To numerically illustrate the reduction step of using the $\bar{\mathbf{M}}$ matrix of Eq. (52), we began by performing a two-term R-matrix calculation including all six $(N+1)$-electron bound CS functions in the set $\{\chi_\alpha\}$, given in Table I. The resulting collision strength for the ^2S partial wave is shown in Fig. 2 as the short-dashed curve. At about 70 eV, there is a large, nonphysical resonance feature, which is due to capture into the $1s2s(^1S)\overline{3s}\ {}^2S$ term; it results from the fact that we did not include the $1s2s\ {}^1S$ term in our close-coupling expansion. An even larger pseudoresonance occurs around 90 eV from capture into the $1s\overline{3s}^2\ {}^2S$ term. We can attempt to remove both of these resonances by omitting the $1s2s(^1S)\overline{3s}\ {}^2S$ and $1s\overline{3s}^2\ {}^2S$ CS functions from the $(N+1)$-electron basis. The result of this two-term calculation

TABLE II. ^2S wave-function description for the $1s2s\ ^3S \rightarrow 1s2s\ ^1S$ transition in Li^+

Target orbitals $P_{n_j\ell_j}$	Target terms in the set $\{\Phi_j\}$	$(N+1)$-electron CS functions in the set $\{\chi_\alpha\}$
$1s$	$1s2s(^3S)$	$1s^2 2s\ ^2S$
$2s$	$(c_1 1s2s + c_2 1s\overline{3s})(^1S)$	$1s^2\overline{3s}\ ^2S$
$\overline{3s}$		$1s2s^2\ ^2S$
		$1s2s(^1S)\overline{3s}\ ^2S$
		$1s2s(^3S)\overline{3s}\ ^2S$
		$1s\overline{3s}^2\ ^2S$

is shown by the long-dashed curve in Fig. 2. The collision strength is now smooth, but peaks in the region of the first pseudoresonance. When we transform the Hamiltonian, retaining only four linear combinations of the set $\{\chi_\alpha\}$, we obtain the solid curve, in which the collision strength is devoid of any resonance features and is smaller in the threshold region than that obtained from the second calculation. All three calculations agree at high energy. Finally, we performed a two-term calculation that employed the proper 2s orbital from a HF calculation on $1s2s\ ^3S$, and no pseudo-orbitals. The result is identical to that shown by the solid curve. This clearly indicates that the orthonormal transformation for the calculation employing the pseudo orbital retains the correct collision strength while removing any sign of pseudoresonances.

B. $1s2s\ ^3S \rightarrow 1s2s\ ^1S$ excitation in Li^+

As a second example, we consider the ^2S partial wave for the $1s2s\ ^3S \rightarrow 1s2s\ ^1S$ excitation in Li^+. While the following is a model calculation including only the $\mathscr{L}=0$ partial wave, neglecting extra channel coupling, it illustrates how pseudo orbitals arise not only from the choice of a poor initial set of orbitals. Rather, they are often required to account for differences between orbitals within a configuration or of different configurations.

We determined the $1s$ and $2s$ orbitals by performing a HF calculation on the $1s2s\ ^3S$ term. However, the $2s$ orbital is not completely appropriate for describing the $1s2s\ ^1S$ term. A separate HF calculation for this term would yield a slightly different $2s$ orbital and, to a lesser extent, a different $1s$ orbital. We can compensate for this slightly inappropriate $2s$ orbital by performing a MCHF calculation, which includes the $1s2s\ ^1S$ and $1s\overline{2s}\ ^1S$ configuration-state functions. The $\overline{3s}$ pseudo orbital differs from a physical $3s$ orbital and the ^1S term is given by the linear combination $c_1 1s2s\ ^1S + c_2 1s\overline{3s}\ ^1S$, with $c_1 = 0.9919$ and $c_2 = -0.1273$.

The target orbitals $P_{n_j\ell_j}$, the target terms included in the close-coupling expansion in Φ_j, and the $(N+1)$-electron bound CS functions χ_α for the ^2S wave-function description are listed in Table II. Again, in this case, $N_c=6$ and $N_r = 3(\text{orbitals}) \times 2(\text{target terms}) = 6$, but now the non-orthonormal form of $\vec{\xi}$ is related to $\vec{\chi}$ by the overlap matrix $\mathbf{M}$

$$\vec{\xi} = \begin{pmatrix} 1s2s(^3S)1s \\ 1s2s(^3S)2s \\ 1s2s(^3S)\overline{3s} \\ (c_1 1s2s + c_2 1s\overline{3s})(^1S)1s \\ (c_1 1s2s + c_2 1s\overline{3s})(^1S)2s \\ (c_1 1s2s + c_2 1s\overline{3s})(^1S)\overline{3s} \end{pmatrix} = \mathbf{M}\vec{\chi} = \begin{pmatrix} -\sqrt{\frac{3}{2}} & 0 & 0 & 0 & 0 & 0 \\ 0 & 0 & \sqrt{\frac{3}{2}} & 0 & 0 & 0 \\ 0 & 0 & 0 & 0 & 1 & 0 \\ \frac{-c_1}{\sqrt{2}} & \frac{-c_2}{\sqrt{2}} & 0 & 0 & 0 & 0 \\ 0 & 0 & \frac{-c_1}{\sqrt{2}} & \frac{-c_2}{2} & \frac{-c_2\sqrt{3}}{2} & 0 \\ 0 & 0 & 0 & c_1 & 0 & \frac{-c_2}{\sqrt{2}} \end{pmatrix} \begin{pmatrix} 1s^2 2s \\ 1s^2\overline{3s} \\ 1s2s^2 \\ 1s2s(^1S)\overline{3s} \\ 1s2s(^3S)\overline{3s} \\ 1s\overline{3s}^2 \end{pmatrix} . \quad (53)$$

Note that if $c_2=0$, row 4 is linearly dependent on row 1 and row 5 is linearly dependent on row 2. Thus, there would be two eigenvalues that are trivially zero, corresponding to the $1s2s(^1S)\overline{3s}$ and $1s\overline{3s}^2$ configurations which would not be required by orthogonality considerations. Thus we could reduce the number of linear combinations of $(N+1)$-electron configurations from $N_r=6$ to $N_r=4$. When we diagonalize the actual matrix $\mathbf{B}=\mathbf{M}\mathbf{M}^T$ for $c_2 \neq 0$, however, the eigenvalues are

$$e_i = (1.999\,98,\ 1.993\,91,\ 1.007\,01,\ 0.992\,987,\ 0.006\,092, 0.000\,024) . \quad (54)$$

The second smallest eigenvalue is associated with an eigenvector dominated by the $1s^2\overline{3s}$ configuration, which lies well below the ground-state continuum, whereas the smallest eigenvalue is associated with an eigenvector dominated by the $1s\overline{3s}^2$ configuration, which gives rise to a pseudoresonance. We only keep four of the possible six linear combinations of the three-electron states χ_α due to the smallness of these last two eigenvalues. The resulting orthonormal $\bar{\mathbf{M}}$ matrix is given by

$$\bar{\mathbf{M}}=\begin{pmatrix} 0.0000 & 0.0000 & -0.9959 & 0.0446 & 0.0782 & 0.0020 \\ -0.9995 & 0.0318 & 0.0000 & 0.0000 & 0.0000 & 0.0000 \\ 0.0000 & 0.0000 & 0.0871 & 0.2558 & 0.9625 & 0.0229 \\ 0.0000 & 0.0000 & -0.0229 & 0.9615 & 0.2597 & -0.0871 \end{pmatrix} . \tag{55}$$

It is interesting to see under which conditions the smallest eigenvalue of the matrix **B** would exceed our cutoff value of 0.01. We artificially increased the exchange potential by a factor of 60 and found the mixing coefficients from a MCHF calculation to be $c_1=0.814$ and $c_2=0.581$, giving rise to a smallest eigenvalue of $e_6\sim 0.01$. The near equality of these two coefficients for this artificial case indicated that there is such strong mixing between the $1s2s(^1S)$ and $1s\overline{3s}(^1S)$ terms that this two-term approximate close-coupling expansion is completely inadequate to begin with. What is more appropriate in such a case is to include the physical $1s3s(^1S)$ term within the close-coupling expansion and to correct for any further term dependence of the $1s2s(^1S)$ term by mixing with a $1s\overline{4s}(^1S)$ pseudoconfiguration. Then the $1s3sn\ell$ resonances will all be real. The $1s\overline{4s}^2$ pseudoresonance, on the other hand, will be associated with an eigenvalue much less than 0.01 and therefore is discarded. For general cases, we find that the size of the small eigenvalues serves as an important diagnostic for determining whether or not the number of terms retained in the close-coupling expansion is adequate.

To illustrate the problem of pseudoresonances in the actual $c_1=0.9919$, $c_2=-0.1273$ case, we first carried out a two-term R-matrix calculation including all six $(N+1)$-electron bound CS functions in the set $\{\chi_\alpha\}$, given in Table II. The resulting collision strength for the ^2S partial wave is shown in Fig. 3 as the short-dashed curve. At about 30–40 eV, there is a huge, nonphysical resonance feature that is due to capture into the $1s\overline{3s}^2\ ^2S$ term. We can attempt to remove this resonance by omitting the $1s\overline{3s}^2\ ^2S$ CS function from the $(N+1)$-electron basis. The result of this calculation yields the long-dashed curve in Fig. 3. We see that the collision strength now is much larger at threshold and shows a zero at about 18 eV, compared to the zero at about 10 eV in the first calculation. We note that this zero is due to cancellation between the $R^0(1s,k_1s;k_2s,1s)$ and $R^0(2s,k_1s;k_2s,2s)$ Slater integrals occurring in the $\mathscr{L}=0$, doublet partial wave only and is therefore not experimentally observable; the greater contributions from higher partial waves mask this behavior in the total cross section. When we transform the Hamiltonian, retaining only four linear combinations of the set $\{\chi_\alpha\}$, we see from the solid curve in Fig. 3 that the collision strength in the threshold region, at the energy of the zero in the collision strength, and in the high-energy region is almost identical to that from the calculation employing all six $(N+1)$-electron bound CS functions. However, the pseudoresonance has disappeared and is now replaced by a smooth curve in this energy region.

We also performed a four-term calculation by including the $1s\overline{3s}\ ^3S$ and $1s\overline{3s}\ ^1S$ terms in the close-coupling expansion of the target. Even though they correspond to unphysical states and are therefore meaningless, their inclusion provides further insight into the nature of the $1s\overline{3s}^2\ ^2S$ pseudoresonance. For this case, we have 12 possible $(N+1)$-electron bound terms contained in $\vec{\xi}$, by orthogonality considerations. However, the first six eigenvalues are identically equal to 2.0 while the second six are identically equal to 0.0. Therefore, as expected, a transformation was not required. The results of this calculation are shown in Fig. 4 by the solid curve. By comparing the nonresonant part of this collision strength to the transformed results (short-dashed curve), we see that the present results do not omit and of the continuum description. We also see that the one huge pseudoresonance has now disappeared and is replaced by a series of pseudoresonances

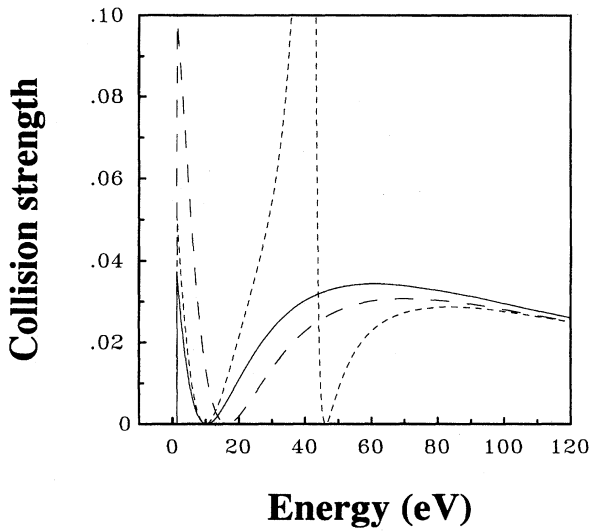

FIG. 3. Electron-impact excitation collision strength for the $1s2s\ ^3S\rightarrow 1s2s\ ^1S$ transition in Li^+ from various two-term R-matrix calculations in the ^2S partial wave. Short-dashed curve, full calculation using all $(N+1)$-electron bound CS functions from Table I; long-dashed curve, calculation omitting just the $1s\overline{3s}^2\ ^2S$ CS function; solid curve, calculation using the transformed, reduced basis set. Again, both the short-dashed curve and the long-dashed curve exhibit unphysical behavior.

TABLE III. ^2D wave-function description for the $3d^{10}4s^2 \rightarrow 3d^9 4s^2 4d$ excitations in Kr^{6+}.

Open-shell target orbitals $P_{n\ell}$	Target terms in the set $\{\Phi_j\}$	$(N+1)$-electron configurations to form the set $\{\chi_\alpha\ (^{2\ell+1}\mathscr{L} = {}^2D)\}$
$3d$	$3d^{10}4s^2(^1S)$	$3d^{10}4s^2 4d$
$4d$	$3d^9 4s^2 4d(^{2S+1}L \neq {}^1S)$	$3d^{10}4s^2\overline{5d}$
$\overline{5d}$	$(c_1 3d^9 4s^2 4d + c_2 3d^9 4s^2\overline{5d})(^1S)$	$3d^9 4s^2 4d^2$
		$3d^9 4s^2 4d\overline{5d}$
		$3d^9 4s^2\overline{5d}^2$

of the form $1s\overline{3s}ns\ ^2S$, whose total contribution to the collision strength is much smaller.

Finally, we show the results of a distorted-wave calculation as the long-dashed curve in Fig. 4; it has similar behavior at the zero and at high energy as the transformed R-matrix results, although the threshold behavior is slightly lower. For the present case of a singly charged target, however, we do not expect the distorted-wave method to reproduce the non-resonant behavior of the R-matrix method. For multiply charged ions, we do expect better agreement. Note that all three curves merge at high energy.

C. $3d^{10}4s^2 \rightarrow 3d^9 4s^2 4d$ excitation in Kr^{6+}

The previous cases in Li^+ are very simple examples of how pseudoresonances arise. However, the same essential features occur in more complex cases such as the $3d^{10}4s^2 \rightarrow 3d^9 4s^2 4d$ excitations in Kr^{6+}. In an earlier study [13], we found that a $\overline{5d}$ pseudo orbital was needed as a term-dependent correction to the $3d^9 4s^2 4d\ ^1S$ term in order to reproduce the measured excitation-autoionization contribution to the electron-impact ionization cross section [20].

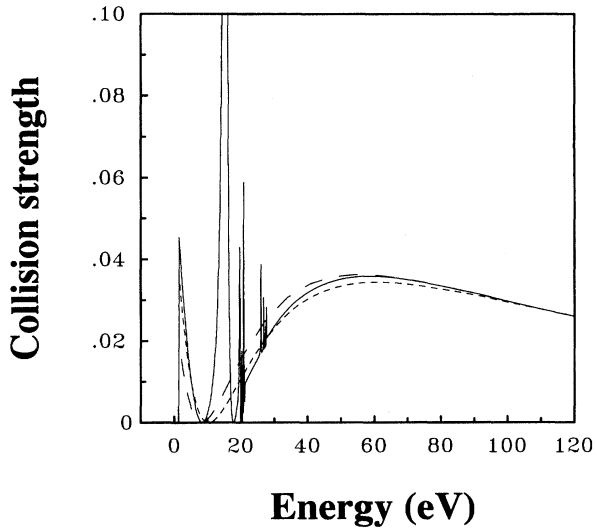

FIG. 4. Electron-impact excitation collision strength for the $1s2s\ ^3S \rightarrow 1s2s\ ^1S$ transition in Li^+ from various calculations in the ^2S partial wave. Short-dashed curve, two-term R-matrix calculation using the transformed, reduced basis set, long-dashed curve, distorted-wave calculation, solid curve; four-term R-matrix calculation using all $(N+1)$-electron bound CS functions from Table I.

Thus this term was described by the weighted sum $(c_1 3d^9 4s^2 4d + c_2 3d^9 4s^2\overline{5d})\ ^1S$, with $c_1 = -0.9626$ and $c_2 = 0.2710$. It was also found in this study, however, that the existence of $3d^9 4s^2\overline{5d}^2$ pseudoresonances led to a severe discrepancy between R-matrix and distorted-wave cross sections. The open-shell target orbitals, the terms included in the close-coupling expansion of the target, and the $(N+1)$-electron bound configurations from which the CS functions χ_α are formed for the ^2D wave-function description are listed in Table III. By noting all couplings of the configurations listed in the third column that can lead to ^2D symmetry, the size of the set of $(N+1)$-electron bound CS functions is found to be $N_c = 22$. Since we include the 11 target terms $3d^{10}4s^2\ ^1S$, $3d^9 4s^2 4d(^3S, {}^{1,3}P, {}^{1,3}D, {}^{1,3}F, {}^{1,3}G)$, and $(c_1 3d^9 4s^2 4d + c_2 3d^9 4s^2\overline{5d})\ ^1S$ and we have three open-shell target orbitals $3d,4d,\overline{5d}$, there are $N_r = 33$ possible coupled terms required by orthogonality. Of these, 11 are trivially zero, so that N_r can be reduced to 22

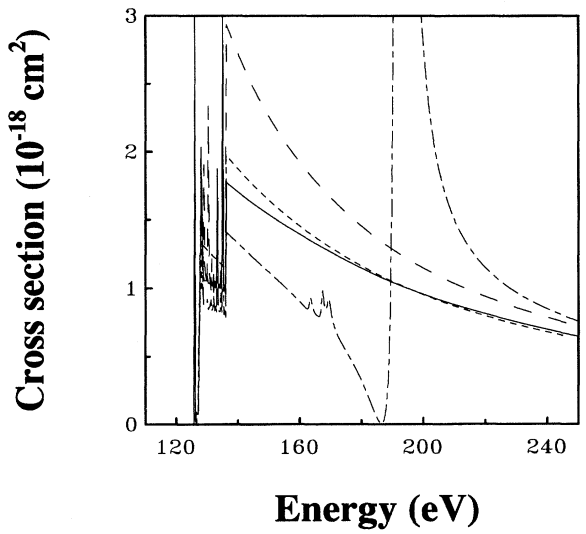

FIG. 5. Electron-impact excitation cross section for the $3d^{10}4s^2 \rightarrow 3d^9 4s^2 4d$ transitions in Kr^{6+} from various calculations in the ^2D partial wave. Long-dash–short-dashed curve, full 11-term R-matrix calculation using all 22 $(N+1)$-electron bound CS functions; long-dashed curve, 11-term R-matrix calculation omitting the five $3d^9 4s^2\overline{5d}^2\ ^2D$ CS functions, short-dashed curve, distorted-wave calculation, solid curve, 11-term R-matrix calculation using the transformed, reduced basis set. The long-dash–short-dashed curve and the long-dashed curve yield total cross sections quite different from the experimental results [20].

immediately. Of these 22 remaining linear combinations of the χ, 17 have eigenvalues between 0.9 and 1.0, and 5 have eigenvalues less than 0.0001. By reducing the size from 22 to 17, we eliminate the pseudoresonances associated with the five $3d^9 4s^2 \overline{5d}^2\ ^2D$ configurations.

The ^2D partial wave cross section is shown in Fig. 5 for a variety of calculations. When all 22 terms in the set $\{\chi_\alpha\}$ are retained, a huge pseudoresonance feature is observed at about 200 eV, with such a broad width that, even at threshold, the cross section is about 20% lower than the distorted-wave calculation. If we simply omit the five $3d^9 4s^2 \overline{5d}^2\ ^2D$ CS functions from the expansion, the cross section is about 50% higher at the final threshold than the distorted-wave cross section. When the reduction step is applied, however, we notice that (i) the pseudoresonance disappears, (ii) the above-all-thresholds cross section is quite similar to the distorted-wave one, (iii) below the ^1S threshold the resonance profile is identical to that from the full calculation using Ψ_S, although the background is higher.

V. SUMMARY

We have developed a transformation of the R-matrix Hamiltonian that is capable of removing the class of pseudoresonances that often occur when the number of terms included in the close-coupling expansion is smaller than the set of terms that can be formed from the configurations included in the configuration-interaction expansion of the target. This is possible with only minor modifications of existing R-matrix programs. We have tested this technique for a wide variety of cases, in addition to the examples included in the present paper. It has proven to be a very efficient method of removing these nonphysical resonances, while preserving the true physical nature of electron-impact excitation cross sections.

ACKNOWLEDGMENTS

We would like to thank the members of the Iron Project for the continued use of their R-matrix programs. T.W.G. and M.S.P. were supported by the U.S. Department of Energy, Office of Fusion Energy, under Contract No. DE-FG05-86-ER53217 with Auburn University; F.R. was supported by the NSF; D.C.G. was supported by the U.S. Department of Energy, Office of Fusion Energy, under Contract No. DE-FG05-93ER54218 with Rollins College; and N.R.B. was supported in part by EPSRC Contract No. GR/K/14346 with the University of Strathclyde.

[1] *Atomic Processes in Plasmas*, edited by W. L. Rowan, AIP Conf. Proc. No. 322 (AIP, New York, 1995).
[2] A. H. Gabriel and C. Jordan, *Case Studies in Atomic Collision Physics II*, edited by M. R. C. McDowell and E. W. McDaniel (North-Holland, Amsterdam, 1972), p. 211.
[3] M. J. Seaton, Proc. R. Soc. London Ser. A **218**, 400 (1953).
[4] P. G. Burke and W. D. Robb, Adv. At. Mol. Phys. **11**, 143 (1975).
[5] P. G. Burke and K. A. Berrington, *Atomic and Molecular Processes: An R-matrix Approach* (IOP, Bristol, 1993).
[6] B. H. Lengsfield III and T. N. Rescigno, Phys. Rev. A **44**, 2913 (1991).
[7] C. W. McCurdy (private communication).
[8] K. A. Berrington, P. G. Burke, A. Hibbert, M. Mohan, and K. L. Baluja, J. Phys. B **21**, 339 (1988).
[9] P. G. Burke, V. M. Burke, and K. M. Dunseath, J. Phys. B **27**, 5341 (1994).
[10] D. C. Griffin, M. S. Pindzola, and N. R. Badnell, J. Phys. B **25**, L605 (1992).
[11] C. Froese Fischer, *The Hartree-Fock Method for Atoms* (Wiley, New York, 1977).
[12] R. D. Cowan, *The Theory of Atomic Structure and Spectra* (University of California Press, Berkeley, 1981).
[13] T. W. Gorczyca, M. S. Pindzola, N. R. Badnell, and D. C. Griffin, Phys. Rev. A **49**, 4682 (1994).
[14] D. C. Griffin, M. S. Pindzola, T. W. Gorczyca, and N. R. Badnell, Phys. Rev. A **51**, 2265 (1995).
[15] T. T. Scholz, J. Phys. B **24** 2127 (1991).
[16] D. W. Norcross, J. Phys. B **2**, 1300 (1969).
[17] C. Froese Fischer, Comput. Phys. Commun. **64**, 369 (1991).
[18] K. A. Berrington, W. B. Eissner, and P. H. Norrington, Comput. Phys. Commun. (to be published).
[19] D. G. Hummer, K. A. Berrington, W. B. Eissner, A. K. Pradhan, H. E. Saraph, and J. A. Tully, Astron. Astrophys. **279**, 298 (1993).
[20] M. E. Bannister, X. Q. Guo, and T. M. Kojima, Phys. Rev. A **49**, 4676 (1994).